INTERNATIONAL JOURNAL FOR NUMERICAL AND ANALYTICAL METHODS IN GEOMECHANICS, VOL. 18, 161–175 (1994)

ON THE INDENTATION OF A POROELASTIC LAYER

A. P. S. SELVADURAI

Department of Civil Engineering and Applied Mechanics,
McGill University, 817 Sherbrooke St, West, Montreal, Quebec, Canada H3A 2K6

AND

Z. Q. YUE

Centre for Surface Transportation Technology, National Research Council, Ottawa, Ontario, Canada K1A 0R6

SUMMARY

The paper examines the axisymmetric contact problem related to the indentation of a fluid saturated poroelastic layer by a smooth rigid punch. The layer rests in bonded contact with a rigid impermeable base and the surface of the layer is considered to be either permeable or impermeable. The paper develops the integral equations governing the problem for the generalized case where the pore fluid exhibits compressibility. The numerical results presented in the paper illustrate the influence of the relative layer thickness, drainage conditions and the compressibility of the pore fluid on the degree of consolidation settlement of the indenting punch.

INTRODUCTION

The one-dimensional theory of the consolidation of a water saturated geomaterial was first developed by Terzaghi[1] and subsequently extended by Biot[2,3] to include three-dimensional deformations of the porous medium and compressibility of the pore fluid. The theory has been successfully applied to the study of various loading and contact problems associated with half-space and infinite-space regions.[4–13] A great majority of these investigations have focused on the evaluation of the time-dependent behaviour of a porous medium which is saturated with an incompressible pore fluid. The consolidation behaviour of the poroelastic layers has also been extensively investigated in the literature in geomechanics.[14–21] The present paper in particular focuses on the axisymmetric indentation of a poroelastic layer saturated with a compressible fluid. The analysis of the mixed boundary value problem related to a poroelastic layer represents a useful engineering application which models the consolidation behaviour of a relatively rigid foundation resting on the surface of a saturated soil layer (Figure 1). The analysis of the indentation problem also examines the role of pore fluid compressibility on the degree of consolidation settlement of the indenting rigid foundation. The contact and drainage boundary at both the surface of the layer and at the base of the layer are represented by plausible conditions which could represent extreme situations encountered in geomechanics problems. For example, the foundation is assumed to be in smooth contact with the poroelastic layer and the entire surface of the layer is assumed to be either fully permeable or fully impermeable with regard to the pore pressure boundary condition. Similarly, the underlying rigid base is assumed to exhibit bonded contact with the poroelastic layer and this interface is also assumed to be impermeable.

CCC 0363–9061/94/030161–15
© 1994 by John Wiley & Sons, Ltd.

Received 17 June 1993
Revised 18 October 1993

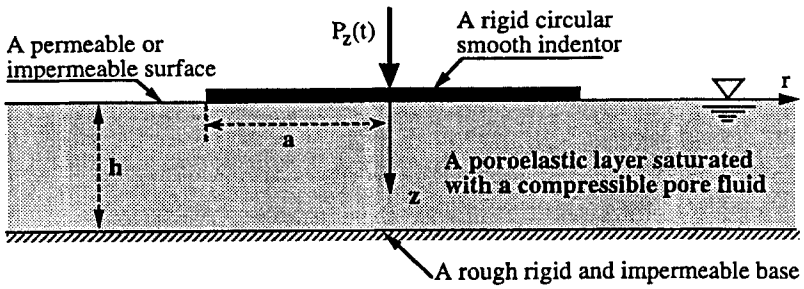

Figure 1. An axisymmetric contact problem in poroelasticity.

The paper presents solution representations governing the poroelastic behaviour of a geomaterial layer containing a compressible fluid and summarizes the integral equations governing the mixed boundary value problems associated with boundary variables represented in a Laplace transform domain. The paper illustrates the influences of the relative thickness of the consolidating layer (i.e. relative to the radius of the foundation), the Poisson ratios associated with the poroelastic medium and the pore pressure boundary conditions on the degree of consolidation settlement of the rigid circular punch.

GOVERNING EQUATIONS

In the following we shall present a brief account of the governing equations referred to a Cartesian tensor notation. The constitutive equations governing the quasi-static response of a poroelastic medium, which consists of an isotropic poroelastic soil skeleton saturated with a compressible pore fluid, take the forms [22,23]

$$\begin{aligned} \sigma_{ij} &= \frac{2\mu\nu}{1-2\nu}\varepsilon_{kk}\delta_{ij} + 2\mu\varepsilon_{ij} - \frac{3(\nu_u-\nu)}{B(1-2\nu)(1+\nu_u)}p\delta_{ij} \\ p &= \frac{2\mu B^2(1-2\nu)(1+\nu_u)^2}{9(\nu_u-\nu)(1-2\nu_u)}\zeta_v - \frac{2\mu B(1+\nu_u)}{3(1-2\nu_u)}\varepsilon_{kk}. \end{aligned} \tag{1}$$

where p is the pore fluid pressure; ζ_v is the volumetric strain in the pore fluid; σ_{ij} is the total stress tensor; ε_{ij} are the soil skeleton strains defined by

$$\varepsilon_{ij} = \tfrac{1}{2}(u_{i,j} + u_{j,i}) \tag{2}$$

and u_i are the corresponding displacement components and the comma denotes a partial derivative with respect to a spatial variable. In the absence of body forces, the quasi-static equations of equilibrium take the form

$$\sigma_{ij,j} = 0 \tag{3}$$

The equation governing quasi-static fluid flow is defined by Darcy's law which takes the form

$$v_i = -\kappa p_{,i} \tag{4}$$

where v_i is the specific discharge vector in the pore fluid. The continuity equation associated with quasi-static fluid flow is

$$\frac{\partial \zeta_v}{\partial t} + v_{i,i} = 0 \tag{5}$$

The above governing equations are characterized by five independent material parameters which are represented by the drained and undrained Poisson ratios ν and ν_u, respectively, the shear modulus μ, Skempton's pore pressure coefficient B and κ ($= k/\gamma_w$, where k is the coefficient of permeability and γ_w is the unit weight of pore fluid). Considering requirements for a positive definite strain energy potential, it can be shown that the material parameters should satisfy the following thermodynamic constraints: $\mu > 0$; $0 \leq B \leq 1$; $-1 < \nu < \nu_u \leq 0{\cdot}5$; $\kappa > 0$.

Based on the theory of Fourier integral transforms,[24] it can be shown that the sets of solution representations exist for the field variables in a linear, isotropic, poroelastic layer of infinite lateral extent, saturated with a compressible pore fluid. In either the temporal domain or the Laplace transform domain and in the cylindrical co-ordinate systems (r, θ, z) and (ρ, φ, z), we have

$$\begin{aligned}
\mathbf{u}(r,\theta,z,t) &= \frac{1}{2\pi}\int_0^\infty\int_0^{2\pi}\frac{1}{\rho}\Pi_a \mathbf{w} K \rho\, d\varphi\, d\rho, & \mathbf{w}(\rho,\varphi,z,t) &= \frac{\rho}{2\pi}\int_0^\infty\int_0^{2\pi}\Pi_a^* \mathbf{u} K^* r\, d\theta\, dr \\
\mathbf{T}_z(r,\theta,z,t) &= \frac{1}{2\pi}\int_0^\infty\int_0^{2\pi}\Pi_a \tau K \rho\, d\varphi\, d\rho, & \tau(\rho,\varphi,z,t) &= \frac{1}{2\pi}\int_0^\infty\int_0^{2\pi}\Pi_a^* \mathbf{T}_z K^* r\, d\theta\, dr \\
\mathbf{v}(r,\theta,z,t) &= \frac{1}{2\pi}\int_0^\infty\int_0^{2\pi}\rho\Pi_a \vartheta K \rho\, d\varphi\, d\rho, & \vartheta(\rho,\varphi,z,t) &= \frac{1}{2\pi\rho}\int_0^\infty\int_0^{2\pi}\Pi_a^* \mathbf{v} K^* r\, d\theta\, dr \\
p(r,\theta,z,t) &= \frac{1}{2\pi}\int_0^\infty\int_0^{2\pi} p_w K \rho\, d\varphi\, d\rho, & p_w(\rho,\varphi,z,t) &= \frac{1}{2\pi}\int_0^\infty\int_0^{2\pi} p K^* r\, d\theta\, dr
\end{aligned} \tag{6a}$$

where $0 \leq z < \infty, 0 < t < \infty$ and the integrals are interpreted in the sense of a Cauchy principal value. The vectors in (6a) are defined by $\mathbf{u} = (u_r, u_\theta, u_z)^T$, $\mathbf{T}_z = (\sigma_{zr}, \sigma_{z\theta}, \sigma_{zz})^T$, $\mathbf{v} = (v_r, v_\theta, v_z)^T$, $\mathbf{w} = (w_1, w_2, w_3)^T$, $\tau = (\tau_1, \tau_2, \tau_3)^T$, and $\vartheta = (\vartheta_1, \vartheta_2, \vartheta_3)^T$. The superscript T stands for the transpose of matrix. K^* and Π_a^* are, respectively, the complex conjugates of the Fourier matrix kernel functions K and Π_a defined by

$$K = e^{+i\rho r\sin(\theta+\varphi)}, \qquad \Pi_a = \begin{pmatrix} +i\sin(\theta+\varphi) & +i\cos(\theta+\varphi) & 0 \\ +i\cos(\theta+\varphi) & -i\sin(\theta+\varphi) & 0 \\ 0 & 0 & 1 \end{pmatrix} \tag{6b}$$

By assuming the initial condition $\zeta_v|_{t=0} = 0$, the governing equations (1)–(5) can be rewritten as two sets of first-order ordinary differential equations in the Fourier and Laplace transform domains; i.e.

$$\frac{d}{dz}\mathbf{V}_v(\rho,\varphi,z,s) = \rho\mathbf{C}_v\mathbf{V}_v(\rho,\varphi,z,s), \qquad \frac{d}{dz}\mathbf{V}_u(\rho,\varphi,z,s) = \rho\mathbf{C}_u\mathbf{V}_u(\rho,\varphi,z,s) \tag{7a}$$

where

$$\mathbf{V}_v = \begin{pmatrix} \hat{w}_2 \\ \frac{1}{\mu}\hat{\tau}_2 \end{pmatrix}, \qquad \mathbf{C}_v = \begin{pmatrix} 0 & 1 \\ 1 & 0 \end{pmatrix}$$

$$\mathbf{V}_u = \begin{pmatrix} \hat{w}_1 \\ \hat{w}_3 \\ \frac{1}{2\mu}\hat{\tau}_3 \\ \frac{1}{2\mu}\hat{\tau}_1 \\ \frac{1}{2\mu\alpha_d}\hat{p}_w \\ \frac{1}{2\mu\kappa\alpha_d}\hat{\vartheta}_3 \end{pmatrix}, \qquad \mathbf{C}_u = \begin{pmatrix} 0 & -1 & 0 & 2 & 0 & 0 \\ \frac{\nu}{1-\nu} & 0 & \frac{1-2\nu}{1-\nu} & 0 & \nu_k & 0 \\ 0 & 0 & 0 & 1 & 0 & 0 \\ \frac{1}{1-\nu} & 0 & \frac{-\nu}{1-\nu} & 0 & \nu_k & 0 \\ 0 & 0 & 0 & 0 & 0 & -1 \\ \gamma^2 - 1 & 0 & 1-\gamma^2 & 0 & -\gamma^2 & 0 \end{pmatrix} \tag{7b}$$

$$\gamma = \sqrt{\frac{1}{c}\frac{s}{\rho^2} + 1}, \qquad c = \frac{2\mu B^2(1-\nu)(1+\nu_u)^2\kappa}{9(\nu_u - \nu)(1-\nu_u)}$$
$$\nu_k = \frac{\nu_u - \nu}{(1-\nu)(1-\nu_u)}, \qquad \alpha_d = \frac{B(1+\nu_u)}{3(1-\nu_u)} \tag{7c}$$

and the superscript $\hat{}$ stands for the Laplace transform with respect to t, and s is the Laplace transform parameter.

By solving the ordinary differential equations, an algebraic solution representation of the field variables in the transform domain can be further obtained in terms of the field variables at the two boundary surfaces of the poroelastic layer as

$$\begin{aligned} 2\mathbf{V}_v(\rho, \varphi, z, s) &= [\mathbf{A}_q e^{-\rho z}]\mathbf{V}_v(\rho, \varphi, 0, s) + [\mathbf{A}_p e^{\rho(z-h)}]\mathbf{V}_v(\rho, \varphi, h, s) \\ 2\mathbf{V}_u(\rho, \varphi, z, s) &= [\mathbf{Q}_q e^{-\rho z} + \mathbf{Q}_t e^{-\rho\gamma z} + \rho z\mathbf{Q}_v e^{-\rho z}]\mathbf{V}_u(\rho, \varphi, 0, s) \\ &\quad + [\mathbf{Q}_p e^{\rho(z-h)} + \mathbf{Q}_s e^{\rho\gamma(z-h)} + \rho(z-h)\mathbf{Q}_u e^{\rho(z-h)}]\mathbf{V}_u(\rho, \varphi, h, s) \end{aligned} \tag{8}$$

where $0 \le z \le h$, the eight coefficient square matrices $\mathbf{A}_p$, $\mathbf{A}_q$, $\mathbf{Q}_p$, etc. are non-dimensional functions of γ (see Appendix A).

By putting $z = 0$ and $z = h$ in equation (8), we can obtain eight independent boundary algebraic equations governing the 16 boundary variables at the two boundary surfaces of the poroelastic layer as

$$\begin{aligned} &[\mathbf{A}_p - \mathbf{A}_q e^{-\rho h}]\mathbf{V}_v(\rho, \varphi, 0, s) + [\mathbf{A}_q - \mathbf{A}_p e^{-\rho h}]\mathbf{V}_v(\rho, \varphi, h, s) = \mathbf{0} \\ &[\mathbf{Q}_p + \mathbf{Q}_s - \mathbf{Q}_q e^{-\rho h} - \mathbf{Q}_t e^{-\rho\gamma h} - \rho h\mathbf{Q}_v e^{-\rho h}]\mathbf{V}_u(\rho, \varphi, 0, s) \\ &+ [\mathbf{Q}_q + \mathbf{Q}_t - \mathbf{Q}_p e^{-\rho h} - \mathbf{Q}_t e^{-\rho\gamma h} + \rho h\mathbf{Q}_u e^{-\rho h}]\mathbf{V}_u(\rho, \varphi, h, s) = 0 \end{aligned} \tag{9}$$

THE INDENTATION PROBLEM

We consider the problem of a rigid circular punch which is in smooth contact with a fluid saturated poroelastic layer and subjected to an axisymmetric load. The poroelastic layer rests on

a rough and impermeable rigid base. The entire upper surface of the poroelastic is assumed to be either completely permeable or completely impermeable (see Fig. 1). For future reference, the mixed boundary conditions at the surface $z = 0$ of the poroelastic layer $0 \leq z \leq h$ are represented in relation to a generalized asymmetric state of deformation as

$$\begin{aligned} u_z(r, \theta, 0, t) &= D_z(r, \theta, t), && 0 \leq r < a \\ \sigma_{zz}(r, \theta, 0, t) &= 0, && a < r < \infty \\ \sigma_{rz}(r, \theta, 0, t) &= 0, && 0 \leq r < \infty \\ \sigma_{\theta z}(r, \theta, 0, t) &= 0, && 0 \leq r < \infty \end{aligned} \tag{9a}$$

where $D_z(r, \theta, t)$ is the prescribed displacement of the rigid circular punch.

The two extreme drainage conditions at the surface $z = 0$ of the poroelastic layer are given by the following cases.

Case I: The surface $z = 0$ of the poroelastic layer is assumed to be a completely previous surface both within and exterior to the punch,

$$p(r, \theta, 0, t) = 0 \tag{9b}$$

Case II: The surface $z = 0$ of the poroelastic layer is assumed to be a completely impervious surface both within and exterior to the punch,

$$v_z(r, \theta, 0, t) = 0 \tag{9c}$$

For a rough rigid and impermeable base, we have the following boundary conditions at the interface $z = h$ of the poroelastic layer and base:

$$u_z(r, \theta, h, t) = 0; \qquad u_r(r, \theta, h, t) = 0; \qquad u_\theta(r, \theta, h, t) = 0; \qquad v_z(r, \theta, h, t) = 0 \tag{9d}$$

where $0 \leq r < \infty$, $0 \leq \theta < 2\pi$ and $0 \leq t < \infty$.

Consequently, we can express $\hat{w}_3(\rho, \varphi, 0, s)$ in terms of $\hat{\tau}_3(\rho, \varphi, 0, s)$ as follows for both Cases I and II.

$$\hat{w}_3(\rho, \varphi, 0, s) = \frac{-1}{\mu} k_0(\gamma, \rho h) \hat{\tau}_3(\rho, \varphi, 0, s) \tag{10a}$$

where $\hat{w}_3$ and $\hat{\tau}_3$ are, respectively, the vertical displacement u_z and normal stress σ_{zz} at $z = 0$ in the transform domain; k_0 can be algebraically evaluated from the boundary equations (8).

By using these expressions and equations (6), we obtain the two-dimensional Fourier transform-based dual integral equations, in the Laplace transform domain, governing the time-dependent behaviour of the smooth rigid circular punch as

For Cases I and II, we have

$$\begin{aligned} \frac{1}{2\pi} \int_0^\infty \int_0^{2\pi} k_0(\gamma, \rho h) \hat{\tau}_3(\rho, \varphi, 0, s) K \, \mathrm{d}\varphi \, \mathrm{d}\rho &= -\mu \hat{D}_z(r, \theta, s), && 0 \leq r \leq a \\ \frac{1}{2\pi} \int_0^\infty \int_0^{2\pi} \hat{\tau}_3(\rho, \varphi, 0, s) K \rho \, \mathrm{d}\varphi \, \mathrm{d}\rho &= 0, && a < r < \infty \end{aligned} \tag{11}$$

where $0 \leq \theta < 2\pi$, $\mathrm{Re}(s) > 0$.

We now reduce the above formulation to the case of an axisymmetric rigid indentor with a flat base, for which $\hat{D}_z(r, \theta, s) = \hat{D}_z(s)$. The 2-D integral equations (11) can be reduced to one-dimensional Hankel transform-based integral equations by using Fourier series expansions (see

e.g. Reference 24). The resulting equations are the following: For Cases I and II, we have

$$\int_0^\infty k_0(\gamma, \rho h)\hat{\tau}_{30}(\rho, s)J_0(\rho r)\,\mathrm{d}\rho = -\mu\hat{D}_z(s), \quad 0 \le r \le a$$
$$\int_0^\infty \hat{\tau}_{30}(\rho, s)J_0(\rho r)\,\mathrm{d}\rho = 0, \qquad a < r < \infty \tag{13a}$$

where J_0 is the Bessel function of order zero.

For the purpose of evaluation of the total force on the indentor, we note that, for the two cases, the unknown contact stress beneath the rigid disc punch can be expressed as follows:

$$\hat{\sigma}_{zz}(r, \theta, 0, s) = \int_0^\infty \hat{\tau}_{30}\,J_0(\rho r)\,\rho\,\mathrm{d}\rho \tag{13b}$$

FREDHOLM INTEGRAL EQUATIONS GOVERNING THE INDENTATION PROBLEM

The sets of Hankel transform-based integral equations (13a) are singular integral equations with unknown singularities. Further simplifications and reductions have to be made to account for the unknown singularities occurring in these integral equations. Isolating these singularities, it is found that the sets of integral equations can be reduced to the systems of Fredholm integral equations of the second kind in the Laplace transform domain. Such systems of complex Fredholm integral equations of the second kind are standard and regular integral equations which can be numerically evaluated (see e.g. References 25–27). Based on the standard procedure (see e.g. Reference 24), we define the following solution representation for $\hat{\tau}_{30}(\rho, s)$ in terms of the auxiliary functions $\hat{\phi}_0(x, s)$:

$$\hat{\tau}_{30}(\rho, s) = \int_0^a \hat{\phi}_0(x, s)\cos(\rho x)\,\mathrm{d}x$$
$$= \frac{1}{\rho}\left\{\hat{\phi}_0(a, s)\sin(\rho a) - \int_0^a \frac{\partial\hat{\phi}_0(x, s)}{\partial x}\sin(\rho x)\,\mathrm{d}x\right\} \tag{14}$$

We also note that

$$\int_0^\infty \hat{\tau}_{30}(\rho, s)J_0(\rho r)\,\mathrm{d}\rho = \int_0^r \frac{\hat{\phi}_0(x, s)}{\sqrt{(r^2 - x^2)}}\,\mathrm{d}x \tag{15}$$

Then the dual integral equations (13a) can be reduced to the integral equation of the Abel type:

$$\int_0^r \frac{\hat{\phi}_0(x, s)}{\sqrt{(r^2 - x^2)}}\,\mathrm{d}x + \int_0^\infty \left[\frac{1}{1-\nu}k_0(\gamma, \rho h) - 1\right]\hat{\tau}_{30}(\rho, s)J_0(\rho r)\,\mathrm{d}\rho = \frac{-\mu}{1-\nu}\hat{D}_z(s) \tag{16}$$

The solution of the Abel-type integral equations (16) can be written as

$$\hat{\phi}_0(r, s) + \int_0^a K_0(r, y, s)\hat{\phi}_0(y, s)\,\mathrm{d}y = \frac{2}{\pi}\left(\frac{-\mu}{1-\nu}\right)\hat{D}_z(s) \tag{17a}$$

where $0 \le r < a$, and the symmetric kernel function $K_0(r, y, s)$ is given below:

$$K_0(r, y, s) = \frac{2}{\pi}\int_0^\infty \left[\frac{1}{1-\nu}k_0(\gamma, \rho h) - 1\right]\cos(\rho r)\cos(\rho y)\,\mathrm{d}\rho \tag{17b}$$

Equations (17) are the Fredholm integral equations of the second kind, in the Laplace transform domain, governing the axisymmetric loading of a smooth rigid circular punch indenting

a saturated poroelastic layer associated with the two drainage conditions (Cases I and II). The transformed value of the total axial load $\hat{P}_z(s)$ can be evaluated in the following form:

$$\hat{P}_z(s) = -\int_0^a \int_0^{2\pi} \hat{\sigma}_{zz}(r, \theta, 0, s)\, r\, \mathrm{d}\theta \mathrm{d}r = -2\pi \int_0^a \hat{\phi}_0(x, s)\, \mathrm{d}x \tag{17c}$$

For convenience, the following non-dimensional variables $\hat{\phi}(x, s_1)$, $\hat{\psi}(x, s_1)$, $\hat{X}_z(s_1)$ and $\hat{Y}_z(s_1)$ are introduced:

$$x = \frac{r}{a}, \qquad b = \frac{h}{a}, \qquad s_1 = \frac{a^2 s}{c}, \qquad \gamma_1 = \sqrt{\left(1 + \frac{s_1}{\rho}\right)}$$
$$\hat{\phi}_0(r, s) = \frac{-P_z}{2\pi a}\hat{\phi}(x, s_1), \qquad \hat{D}_z(s) = \frac{1 - \nu}{4\mu a} P_z \hat{X}_z(s_1), \qquad \hat{P}_z(s) = P_z \hat{Y}_z(s_1) \tag{18}$$

We then obtain the Fredholm integral equation of the second kind in the following non-dimensional forms:

For Cases I and II, we have

$$\hat{\phi}(x, s_1) + \int_0^1 \hat{K}(x, y, s_1)\, \hat{\phi}(y, s_1)\, \mathrm{d}y = \hat{X}_z(s_1) \tag{19a}$$

where $0 \leq x \leq 1$; and the kernel function, $\hat{K}_1$, is given in the following non-dimensional form:

$$\hat{K}(x, y, s_1) = \frac{2}{\pi}\int_0^\infty \left[\frac{1}{1 - \nu} k_0(\gamma_1, \rho b) - 1\right] \cos(\rho x) \cos(\rho y)\, \mathrm{d}\rho \tag{19b}$$

It can be shown that the infinite integrals in equations (19b) with the independent variables x, y and s_1 are uniformly and absolutely convergent provided $\mathrm{Re}(s_1) > 0$. Equation (17c) can be reduced to

$$\int_0^1 \hat{\phi}(x, s_1)\, \mathrm{d}x = \hat{Y}_z(s_1) \tag{19c}$$

The contact normal stress in the Laplace transform domain can be expressed in terms of the auxiliary function $\hat{\phi}(x, s)$ for the rigid circular indentor problem associated with Cases I and II:

$$\hat{\sigma}_{zz}(r, \theta, 0, s_1) = \frac{-P_z}{\pi a^2}\left[\frac{\hat{\phi}(1, s_1)}{\sqrt{(1 - r^2)}} - \int_r^1 \frac{\partial \hat{\phi}(x, s_1)}{\partial x} \frac{\mathrm{d}x}{\sqrt{(x^2 - r^2)}}\right] \tag{19d}$$

where $0 \leq r < 1$.

INTEGRAL EQUATIONS FOR LIMITING CONDITIONS

It is instructive to first examine the limiting cases which pertain to the initial response as $t \to 0^+$, the final response as $t \to +\infty$ and the limiting case as $h \to +\infty$. In particular, we have the following limits,

$$\lim_{s \to \infty} k_0(\gamma, \rho h) = (1 - \nu_u)[k_r(\rho h, \nu_u) + 1]$$
$$\lim_{s \to +0} k_0(\gamma, \rho h) = (1 - \nu)[k_r(\rho h, \nu) + 1] \tag{20a}$$
$$\lim_{h \to \infty}\left[\frac{1}{1 - \nu} k_0(\gamma, \rho h) - 1\right] = \frac{\alpha_1}{2} k_h(\gamma)$$

where

$$k_r(y,\chi) = -\frac{2[(1-\alpha^2)e^{-4y} + [1+\alpha^2+2(1-\alpha)^2(1+y)y]e^{-2y}]}{(1-\alpha^2)(1+e^{-2y})^2 + 4[\alpha^2+(1-\alpha)^2y^2]e^{-2y}}$$

$$k_h(\gamma) = \begin{cases} \dfrac{1-\gamma}{\gamma+1-\alpha_1} & \text{for Case I} \\ \dfrac{2-\gamma(\gamma+1)}{\gamma(\gamma+1)-\alpha_1} & \text{for Case II} \end{cases} \tag{20b}$$

$$\alpha = \frac{1-2\chi}{2(1-\chi)}, \qquad \alpha_1 = \frac{2(\nu_u - \nu)}{1-\nu}$$

Then we have the Fredholm integral equations of the second kind governing the following limiting responses of the rigid circular punch:

(i) For the initial case as $t \to 0^+$, we have

$$\phi_0(r,0^+) + \int_0^a K_1(r,y,\nu_u)\,\phi_0(y,0^+)\,dy = \frac{2}{\pi}\left(\frac{-\mu}{1-\nu_u}\right)D_z(0^+) \tag{21a}$$

(ii) For the final case as $t \to \infty$, we have

$$\phi_0(r,\infty) + \int_0^a K_1(r,y,\nu)\,\phi_0(y,\infty)\,dy = \frac{2}{\pi}\left(\frac{-\mu}{1-\nu}\right)D_z(\infty) \tag{21b}$$

where $0 \le r < a$, and the symmetric kernel function in the integral equations (21a) and (21b) is given by

$$K_1(r,y,\chi) = \frac{2}{\pi}\int_0^\infty k_r(\rho h,\chi)\cos(\rho r)\cos(\rho y)\,d\rho \tag{21c}$$

(iii) For the limiting case as $h \to \infty$, we have,

$$\hat{\phi}_0(r,s) + \int_0^a K_2(r,y,s)\,\hat{\phi}_0(y,s)\,dy = \frac{2}{\pi}\left(\frac{-\mu}{1-\nu}\right)\hat{D}_z(s) \tag{22a}$$

where $0 \le r < a$, and the symmetric kernel function $K_2(r,y,s)$ is given by

$$K_2(r,y,s) = \frac{\alpha_1}{\pi}\int_0^\infty k_h(\gamma)\cos(\rho r)\cos(\rho y)\,d\rho \tag{22b}$$

NUMERICAL SOLUTIONS FOR THE INTEGRAL EQUATIONS

Considering the structure of the kernel function (19b), it becomes evident that the systems of Fredholm integral equations of the second kind have no known exact solution. In this paper, we adopt the following numerical scheme for the evaluation of time-dependent solutions of the integral equations in the Laplace transform domain. First, we separate the complex variables in the integral equations into their real and imaginary parts. We then obtain new systems of Fredholm integral equations of the second kind associated with real variables. Secondly, we divide the interval $[0,1]$ into N segments with ends defined by $r_k = (k-1)/N$, $k = 1,2,3,\ldots,(N+1)$. The collocation points are $x_k = (r_k + r_{k+1})/2$, $k = 1,2,3,\ldots,N$. Consequently, we can convert the integral equations into the systems of linear algebraic equations.

These linear algebraic equations can be written in a generalized matrix form as

$$\sum_{j=1}^{2N+2} [\mathbf{A}_{lj}]\{\hat{\mathbf{X}}_j\} = \{\mathbf{B}_l\}, \quad l = 1, 2, 3, \ldots, 2N + 2 \tag{23}$$

The matrix equation (23) can be solved numerically to generate the unknown variables $\hat{\phi}(x_l, s_1)$ and $\hat{X}_z(s_1)$ (or $Y_z(s_1)$) in the Laplace transform domain. The time-dependent results of the variables can be evaluated by using a modified algorithm for inverse Laplace transforms. This modified algorithm is based on the work of Crump[28] and Talbot[29] and the details are given by Yue.[30]

The numerical techniques adopted here involve three computational steps which are essentially based on repeated numerical integrations. The first step involves the numerical integration of the infinite integrals, which occur in the kernel function (19b). As noted previously, these infinite integrals are uniformly convergent. However, there are two unusual aspects in the numerical integrations. The first refers to the infinite limit and the second is associated with the integrands. As the values of the independent variables s and ρ become large, the integrands will become rapidly oscillatory functions. This property of the integrands will slow the convergence of the numerical integration and render the numerical integration procedure unstable. Large values of the complex variable s are associated with small values of t in the numerical inversion of Laplace transforms. The technique adopted in this study overcomes these two numerical problems. This particular technique consists of an approximation technique and a proceeding limit technique. In the approximation technique, the integrands are separated into two parts. One deals with their asymptotic behaviour as $s_1/\rho^2 \to 0$. The other is the difference between the integrands and their asymptotic functions. Closed-form results can be obtained for the infinite integrals associated with the asymptotic functions. The proceeding limit technique, based on an adaptively iterative Simpson's quadrature, is used for the evaluation of the infinite integrals associated with the remaining terms. The second repeated numerical integration involves systems of Fredholm integral equations, the numerical solution of which has been well investigated by many researchers (e.g. Reference 27). These studies show that with the increase in the segment number N, it is possible to obtain more accurate and readily convergent solutions for the integral equations. The last computational step involves the numerical inversion of Laplace transforms. Due to the accumulation of errors in each repeated numerical integration, however, it is necessary to evaluate and test the convergence and accuracy of the time-dependent results for the systems of Fredholm integral equations of the second kind in the Laplace transform domain. The details of these calculations are documented by Yue.[30] It is concluded from this verification that the numerical scheme and techniques adopted in this study provide highly stable and accurate solutions in the time domain for the systems of Fredholm integral equations of the second kind in the Laplace transform domain and that these procedures particularly overcome the numerical problems customarily associated with the numerical evaluation of the initial stages of the consolidation of the poroelastic medium.

Finally, although the indentation problem related to a poroelastic medium has been treated in the literature, there is a scarcity of numerical results which can be used to assess both the influences of the undrained compressibility and the accuracy of the numerical schemes adopted in the solution of the governing equations. As an alternative, we adopt here the numerical results given by Chiarella and Booker[9] for the smooth indentation at the completely permeable surface ($0 \leq r < +\infty, z = 0$) of a poroelastic half-space saturated with an incompressible fluid ($\nu_u = 0.5$). (These results are estimated from Figure 2 given by Chiarella and Booker[9]). Table I illustrates the comparison of results for the cases where $\nu_u = 0{\cdot}5$ and $\nu = 0{\cdot}0, 0{\cdot}1, 0{\cdot}2, 0{\cdot}3$ or $0{\cdot}4$. As is evident, the trends indicated by the results of the current study are consistent with the results obtained by Chiarella and Booker.[9]

Table I. A comparison between the degrees of consolidation settlement given by (1) the current study and (2) Chiarella and Booker[9] ($\nu_u = 0{\cdot}5$)

	$\nu = 0{\cdot}0$		$\nu = 0{\cdot}1$		$\nu = 0{\cdot}2$		$\nu = 0{\cdot}3$		$\nu = 0{\cdot}4$	
$\sqrt{(ct/a^2)}$	(1)	(2)	(1)	(2)	(1)	(2)	(1)	(2)	(1)	(2)
0·2	0·250	0·230	0·267	0·257	0·287	0·285	0·310	0·314	0·339	0·359
0·4	0·412	0·384	0·433	0·414	0·456	0·448	0·483	0·483	0·513	0·517
0·6	0·529	0·509	0·550	0·543	0·572	0·569	0·597	0·603	0·625	0·647
0·8	0·614	0·603	0·633	0·630	0·653	0·655	0·675	0·670	0·700	0·716
1·0	0·676	0·655	0·692	0·690	0·710	0·709	0·730	0·743	0·751	0·770
1·2	0·722	0·707	0·737	0·733	0·752	0·750	0·770	0·776	0·788	0·836
1·4	0·757	0·741	0·770	0·762	0·784	0·779	0·800	0·810	0·816	0·845

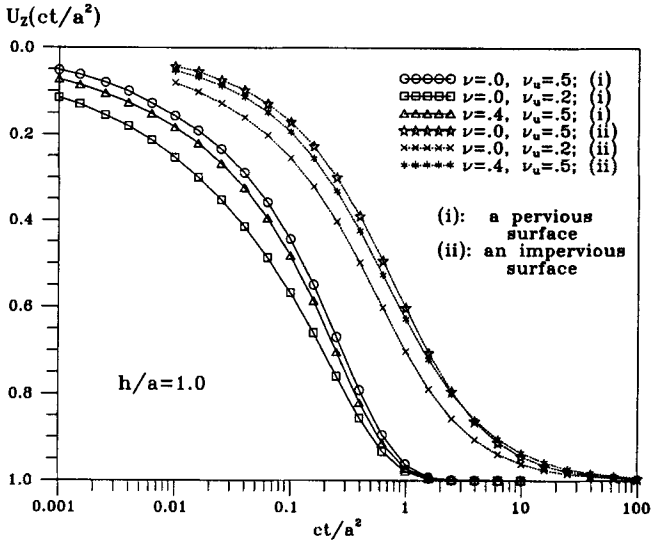

Figure 2. Effect of Poisson's ratios and surface drainage on the degree of consolidation induced axial displacement of the rigid punch.

NUMERICAL RESULTS

The numerical results of primary interest to geomechanical applications relate to the evaluation of the degree of consolidation induced settlement experienced by the rigid circular punch which is subjected to an external load of the form

$$P_z(t) = P_z H(t) \tag{24}$$

where $H(t)$ is the Heaviside step function. The resulting time-dependent rigid displacement of the circular punch is denoted by $D_z(t)$. The degree of consolidation induced displacement of the rigid punch is defined by

$$U_z(t) = \frac{D_z(t) - D_z(0)}{D_z(\infty) - D_z(0)} \tag{25}$$

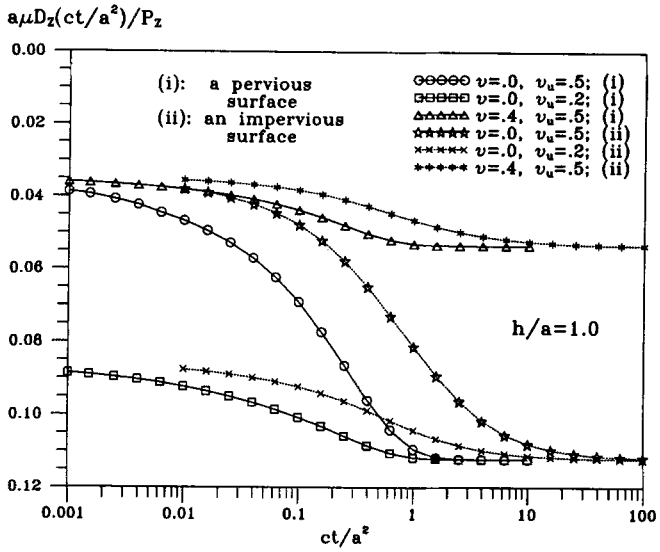

Figure 3. Effect of Poisson's ratios and surface drainages on the consolidation induced axial displacement of the rigid punch.

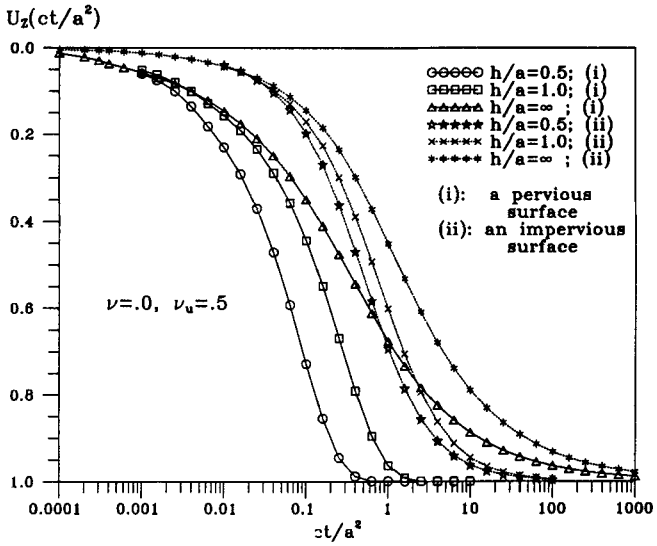

Figure 4. Effect of layer thickness on the degree of consolidation induced axial displacement of the rigid punch.

The initial and final settlements $D_z(0)$ and $D_z(\infty)$ are evaluated by using the limiting equations (21). The non-dimensional time factor ct/a^2 is used in the presentation of the numerical results.

Figures 2 and 3 illustrate the influence of the drained and undrained Poisson's ratios (ν and ν_u) on the rate and magnitude of the consolidation induced displacement of the rigid punch associated with a poroelastic layer with either a pervious surface or an impervious surface. Several combinations of ν and ν_u which represent either realistic estimates of ν for typical

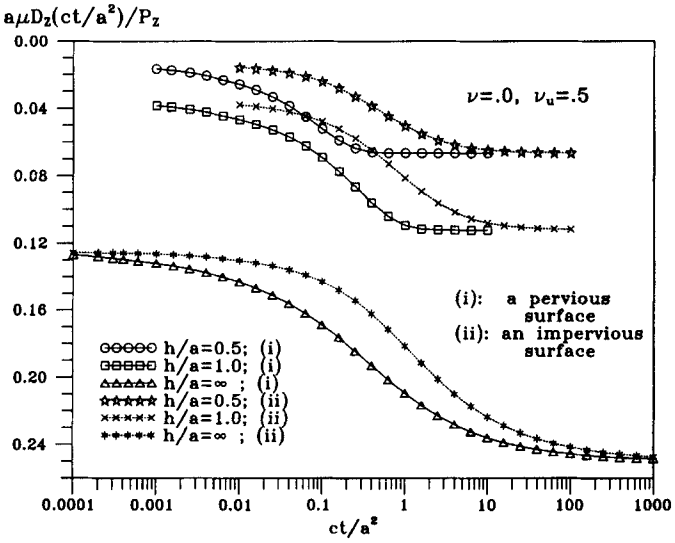

Figure 5. Effect of layer thickness on the consolidation induced axial displacement of the rigid punch.

geomaterials or the extreme limits for compressibility in the undrained response were used. These results are applicable for $h/a = 1$. These figures show that the difference between the undrained and drained Poisson ratios plays a key role in the consolidation induced displacement of the punch.

Figures 4 and 5 illustrate the influence of the poroelastic layer thickness (h/a) on the rate and magnitude of the consolidation induced displacement of the rigid punch. These figures indicate that the rate of consolidation induced axial displacement of the punch increases with the decrease of the layer thickness (h/a), while the magnitude of the consolidation induced displacement of the punch decreases with decrease in the layer thickness.

CONCLUSIONS

The mathematical theory of poroelasticity has been successfully applied to examine the axisymmetric consolidation response of a layer which is indented by a rigid circular indentor with a flat base. It is shown that the mathematical developments associated with mixed boundary value problems can be reduced to Fredholm integral equations of the second-kind in the Laplace transform domain. These equations are amenable to numerical solution and such solutions can be used to develop results of engineering interest. It is shown that the undrained Poisson's ratio of the poroelastic medium has a significant influence on both the magnitude and the rate of the consolidation of the rigid circular indentor. The numerical results also indicate that the relative thickness of the layer (h/a) and the drainage conditions also have a significant influence on the magnitude of the consolidation settlement.

ACKNOWLEDGEMENTS

The work described in this paper was supported by a Natural Sciences and Engineering Research Council of Canada Grant A3866 awarded to A. P. S. Selvadurai. The authors would like to thank the referees for their constructive comments which enhanced the presentation of the material.

APPENDIX A: THE MATRICES IN THE SOLUTION REPRESENTATION

$$\mathbf{Q}_p = \begin{pmatrix} 1 & -\nu_m & 0 & 1+\nu_m & 0 & 0 \\ -\nu_m & 1 & 1+\nu_m & 0 & 0 & 0 \\ 0 & 1-\nu_m & 1 & \nu_m & 0 & 0 \\ 1-\nu_m & 0 & \nu_m & 1 & 0 & 0 \\ 1 & -1 & -1 & 1 & 0 & 0 \\ -1 & 1 & 1 & -1 & 0 & 0 \end{pmatrix} + \alpha_c \begin{pmatrix} 1 & -1 & -1 & 1 & -1 & 1 \\ 1 & -1 & -1 & 1 & -1 & 1 \\ 1 & -1 & -1 & 1 & -1 & 1 \\ 1 & -1 & -1 & 1 & -1 & 1 \\ 0 & 0 & 0 & 0 & 0 & 0 \\ 0 & 0 & 0 & 0 & 0 & 0 \end{pmatrix}$$

$$\mathbf{Q}_q = -\begin{pmatrix} -1 & -\nu_m & 0 & 1+\nu_m & 0 & 0 \\ -\nu_m & -1 & 1+\nu_m & 0 & 0 & 0 \\ 0 & 1-\nu_m & -1 & \nu_m & 0 & 0 \\ 1-\nu_m & 0 & \nu_m & -1 & 0 & 0 \\ -1 & -1 & 1 & 1 & 0 & 0 \\ -1 & -1 & 1 & 1 & 0 & 0 \end{pmatrix} + \alpha_c \begin{pmatrix} 1 & 1 & -1 & -1 & -1 & -1 \\ -1 & -1 & 1 & 1 & 1 & 1 \\ 1 & 1 & -1 & -1 & -1 & -1 \\ -1 & -1 & 1 & 1 & 1 & 1 \\ 0 & 0 & 0 & 0 & 0 & 0 \\ 0 & 0 & 0 & 0 & 0 & 0 \end{pmatrix}$$

$$\mathbf{A}_p = \begin{pmatrix} 1 & 1 \\ 1 & 1 \end{pmatrix}, \quad \mathbf{Q}_s = \begin{pmatrix} -\alpha_c & \frac{1}{\gamma}\alpha_c & \alpha_c & \frac{-1}{\gamma}\alpha_c & \alpha_c & \frac{-1}{\gamma}\alpha_c \\ -\gamma\alpha_c & \alpha_c & \gamma\alpha_c & -\alpha_c & \gamma\alpha_c & -\alpha_c \\ -\alpha_c & \frac{1}{\gamma}\alpha_c & \alpha_c & \frac{-1}{\gamma}\alpha_c & \alpha_c & \frac{-1}{\gamma}\alpha_c \\ -\gamma\alpha_c & \alpha_c & \gamma\alpha_c & -\alpha_c & \gamma\alpha_c & -\alpha_c \\ -1 & \frac{1}{\gamma} & 1 & \frac{-1}{\gamma} & 1 & \frac{-1}{\gamma} \\ \gamma & -1 & -\gamma & 1 & -\gamma & 1 \end{pmatrix}$$

$$\mathbf{A}_q = \begin{pmatrix} 1 & -1 \\ -1 & 1 \end{pmatrix}, \quad \mathbf{Q}_t = \begin{pmatrix} -\alpha_c & \frac{-1}{\gamma}\alpha_c & \alpha_c & \frac{1}{\gamma}\alpha_c & \alpha_c & \frac{1}{\gamma}\alpha_c \\ \gamma\alpha_c & \alpha_c & -\gamma\alpha_c & -\alpha_c & -\gamma\alpha_c & -\alpha_c \\ -\alpha_c & \frac{-1}{\gamma}\alpha_c & \alpha_c & \frac{1}{\gamma}\alpha_c & \alpha_c & \frac{1}{\gamma}\alpha_c \\ \gamma\alpha_c & \alpha_c & -\gamma\alpha_c & -\alpha_c & -\gamma\alpha_c & -\alpha_c \\ -1 & \frac{-1}{\gamma} & 1 & \frac{1}{\gamma} & 1 & \frac{1}{\gamma} \\ -\gamma & -1 & \gamma & 1 & \gamma & 1 \end{pmatrix}$$

$$\mathbf{Q}_u = (1 - \nu_m)\begin{pmatrix} 1 & -1 & -1 & 1 & 0 & 0 \\ 1 & -1 & -1 & 1 & 0 & 0 \\ 1 & -1 & -1 & 1 & 0 & 0 \\ 1 & -1 & -1 & 1 & 0 & 0 \\ 0 & 0 & 0 & 0 & 0 & 0 \\ 0 & 0 & 0 & 0 & 0 & 0 \end{pmatrix}, \quad \mathbf{Q}_v = (1 - \nu_m)\begin{pmatrix} -1 & -1 & 1 & 1 & 0 & 0 \\ 1 & 1 & -1 & -1 & 0 & 0 \\ -1 & -1 & 1 & 1 & 0 & 0 \\ 1 & 1 & -1 & -1 & 0 & 0 \\ 0 & 0 & 0 & 0 & 0 & 0 \\ 0 & 0 & 0 & 0 & 0 & 0 \end{pmatrix}$$

$$\alpha_c = \frac{\nu_u - \nu}{(1 - \nu)(1 - \nu_u)}\left(\frac{1}{\gamma^2 - 1}\right), \qquad \nu_m = \frac{1 - 2\nu_u}{2(1 - \nu_u)}$$

REFERENCES

1. K. Terzaghi, *Erdbaumechanik auf bodenphysikalischer Grundlage*, Franz Deuticke, Leipzig, 1925.
2. M. A. Biot, 'General theory of three-dimensional consolidation', *J. Appl. Phys.*, **12,** 155–164 (1941).
3. M. A. Biot, 'General solution of the equations of elasticity and consolidation for a porous material', *J. Appl. Mech.*, **23,** 91–95 (1956).
4. M. A. Biot and F. M. Clingan, 'Bending settlement of a slab resting on a consolidating foundation', *J. Appl. Phys.*, **13,** 35–40 (1942).
5. J. McNamee and R. E. Gibson, 'Displacement functions and linear transforms applied to diffusion through porous elastic media', *Q. J. Mech. Appl. Math.*, **13,** 98–111 (1960).
6. J. McNamee and R. E. Gibson, 'Plane strain and axially symmetric problems of consolidation of a semi-infinite clay stratum', *Q. J. Mech. Appl. Math.*, **13,** 210–227 (1960).
7. R. L. Schiffman and A. A. Fungaroli, 'Consolidation due to tangential loads', *Proc. 6th. Int. Conf. Soil Found. Eng.*, Montreal, Canada, Vol. 1, (1965) pp. 188–192.
8. L. K. Agbezuge, and H. Deresiewicz, On the indentation of a consolidating half-space, *Israel J. Technol.* **12,** 322–338 (1974).
9. .C. Chiarella and J. R. Booker, 'The time-settlement behavior of a rigid die resting on a deep clay layer', *Q. J. Mech. Appl. Math.*, **28,** 317–328 (1975).
10. L. K. Agbezuge and H. Deresiewicz, 'The consolidation settlement of a circular footing', *Israel J. Technol.* **13,** 264–269 (1975).
11. G. Szefer and J. Gaszynski, 'Axisymmetric punch problem under condition of consolidation', *Archiwum Mechaniki Stosowanej*, **27,** 497–515 (1975).
12. J. Gaszynski and G. Szefer, 'Axisymmetric problem of the punch for the consolidating semi-space with mixed boundary permeability conditions', *Archiwum Mechaniki Stosowanej*, **30,** 17–26 (1978).
13. J. C. Small, 'The time-settlement behaviour of rafts of finite flexibility', *Proc. 4th Australia-New Zealand Conf. Geomech.* Perth, 1984, pp. 159–164.
14. R. E. Gibson, R. L. Schiffman and S. L. Pu, 'Plane strain and axially symmetric consolidation of a clay layer on a smooth impervious base', *Q. J. Mech. Appl. Math.*, **23,** 505–520 (1970).
15. J. R. Booker, 'The consolidation of a finite layer subject to surface loading', *Int. J. Solids Structures*, **10,** 1053–1065 (1974).
16. J. R. Booker and J. C. Small, 'Finite layer analysis of consolidation I', *Int. j. numer. anal. methods geomech.*, **6,** 151–171 (1982).
17. J. R. Booker and J. C. Small, 'Finite layer analysis of consolidation II', *Int. j. numer. anal. methods geomech.*, **6,** 173–194 (1982).
18. J.R. Booker and J.C. Small, 'The time-behaviour of a circular raft of finite flexibility on a deep clay layer', *Int. j. numer. anal. methods geomech.*, **8,** 343–357 (1984).
19. J. R. Booker and J. C. Small, 'A method of computing the consolidation behaviour of layered soils using direct numerical inversion of Laplace transforms', *Int. j. numer. anal. methods geomech.*, **11,** 363–380 (1987).
20. I. Vardoulakis and T.Harnpattanapanich, 'Numerical Laplace–Fourier transform inversion technique for layered-soil consolidation problems: I fundamental solutions and validation', *Int. j. numer. anal. methods geomech.*, **10,** 347–365 (1986).
21. T. Harnpattanapanich, and I. Vardoulakis, 'Numerical Laplace–Fourier transform inversion technique for layered-soil consolidation problems: II. Gibson soil layer', *Int. j. numer. anal. methods geomech.*, **11,** 103–112 (1987).
22. J. R. Rice and M. P. Cleary, 'Some basic stress diffusion solutions for fluid-saturated elastic porous media with compressible constituents', *Rev. Geophys. Space Phys.*, **14,** 227–241 (1976).
23. A. H. D. Cheng and M. Predeleanu, 'Transient boundary element formulation for linear porous-elasticity with applications to soil consolidation', *Appl. Math. Model.*, **11,** 285 (1987).

24. I. N. Sneddon, *The Use of Integral Transforms*, McGraw-Hill, New York, 1972.
25. R. P. Kanwal, *Linear Integral equations: Theory and Technique*, Academic Press, New York, 1971.
26. K. Atkinson, '*A Survey of Numerical Methods for the Solution of Fredholm Integral Equations Of the Second-Kind*', Soc. Industrial and Appl. Math., Philadelphia, PA, 1976.
27. C. T. H. Baker, *The Numerical Treatment of Integral Equations*, Clarendon Press, Oxford, 1977.
28. K. S. Crump, 'Numerical inversion of Laplace transforms using a Fourier series approximation', *J. Assoc. Comp. Machin.*, **10**, 311–327 (1976).
29. A. Talbot, 'The accurate numerical inversion of Laplace transforms', *J. Inst. Math. Appl.* **23**, 97–120 (1979).
30. Z. Q. Yue, 'Mechanics of rigid disc inclusions in fluid saturated poroelastic media', *Ph.D. Thesis*, Carleton University, Ottawa, Canada, 1992.